Designing Interpretable Chess Engines Using Neurosymbolic Methods

May 13, 2022

Abstract

The problem of interpretability in DNNs is classically a hard one, as the parameterisation of perceptron layers is hard to intuit. This paper uses neurosymbolic methods, namely Logical Neural Networks (LNNs), which encode boolean values using Real Logic, to construct an interpretable model for use cases which are easily modelled by logical statements, and applies this architecture to the problem of learning Chess.

Contents

Chapter 1

Interpretability

1.1 Introduction

Research into problems in Machine Learning in recent years has focused largely into using Neural Network (NN) models to solve increasingly broad categories of problems. NNs, much like many other models, define a hypothesis class of functions which differ only in their parameterisation, and uses Stochastic Gradient Descent (SGD) or some descendant thereof, to optimise said parameters given a loss function. Classical Multi-Layer Perceptrons (MLPs) consist of a series of linear layers separated by some non-linearity, (e.g. ReLU, Sigmoid functions). Given certain conditions, it is known that MLPs can learn any continuous function to arbitrary precision, by the Universal Approximation Theorem (UAT). The effectiveness of SGD methods allows us to learn arbitrary functions tractably given sufficient data, which has resulted in a widespread adoption of the architecture in practical settings.

A common criticism of NNs, however, is that they are considered "black box" functions. NNs are difficult to interpret, making it even more difficult to diagnose issues that may arise in production. A particular node in the network may be considered as capturing a single "concept", which can further be used to determine the presence of other concepts. It is difficult, however, to interpret how these concepts are generated - taking linear combinations of features and then applying a non-linear map to the result is not a terribly human line of thinking when it comes to pattern recognition. In this way, when comparing NNs to real-world neural processes, the description of NNs capturing general human intuition, rather than any kind of conscious reasoning, is most apt.

The "black box" nature of NNs has resulted in a hesitancy for it's adoption in particular settings, most notably in the medical industry, where even small risks of misdiagnosis cannot be tolerated. One would assume that an architecture that is so widely used in so many sensitive settings should be easily examinable, but this isn't that case.

From this, the notion of "interpretability" is often discussed when developing or analysing novel neural architectures [21], [2], [5]. An ideal interpretable model would allow the user to know precisely what the model is achieving by arriving at a particular optimal parameterisation. Interpretability is not a quantifiable metric - the user may gain an understanding through a mixture of the learnt parameters and an existing intuition over the architecture itself. This allows for a wide breadth in methods which may be used to gain an understanding of a model, and also hopefully the underlying problem.

1.2 Interpretation Methods

There are many ways we may attempt to approach the problem of interpretability. Commonly used methods take arbitrary NN architectures, and attempt to gauge how relevant a particular feature of a given input is in the overall output of the model. These are known as *Variable Importance Measures* (VIMs). Gradient-based attribution methods [2] are the classical example, where the gradient of the model with respect to its input features are used as the measure of feature importance. This makes intuitive sense, as if the output of the model is subject to large changes with small deviations in an input feature, it must naturally be fairly important. The most commonly seen setting for these methods is in image classification, where the importance of a particular pixel measures how much of an influence said pixel has on determining the category of an image. Plotting the importance of all the pixels

hopefully shows the user precisely which portions of the image contain the relevant object to classification. E.g., distinguishing between cats and dogs would largely rely on examining particular features of the face shape, so one would expect these features to be the most important by this metric.

These methods are very versatile, as they are *model-agnostic*. There are many flaws, however - what if the classification of an image relies on a combination of features, rather than just a single one? We can capture this notion by instead using VIMs over all nodes in the network, i.e. the input layers and all hidden layers, but we run into the same problem - if we determine that a node in a hidden layer is important, how do we begin to understand what this node is doing? This method captures relevance, but does not capture what concepts these features may represent - we can leave this again up to the intuition of the user, or we can apply VIMs recursively between the input features and the hidden feature. This eventually becomes somewhat unwieldy.

Another issue is that VIMs are *local* interpretation methods, as they do not describe the model as a whole - only the model given a set input. This does not give us a good understanding as to why the model's solution to a problem is best.

A solution to the problem of not capturing feature relationships is in developing *model-specific* methods of interpretability. We can design an architecture which allows for novel ways of visualising model behaviour, often by restricting the expressiveness of the model in a manner which allows the remaining hypothesis class to be easily distinguishable.

One example of such an architecture are Neural Additive Models (NAMs) [1]. Neural Additive Models are a generalisation of General Additive Models (GAMs) in that they are fully described by the equation

$$M(\mathbf{x}) = \sigma\left(\sum_i M_i(x_i)\right)$$

Where the $M_i : \mathbb{R} \mapsto \mathbb{R}$ represent univariate NNs, and σ is the *link function*.

In backpropagation, we learn the parameters of each subnetwork M_i simultaneously. Given that each subnetwork is a map $\mathbb{R} \to \mathbb{R}$, we can capture the behaviour of the model not only locally through VIMs, but globally, as we can easily plot the value of M_i over the entire domain. Simply observing this graph allows the user to speculate as to what the model has learnt.

This model, while very interpretable, is not very expressive - we cannot capture any relationships between variables that aren't described by the link function σ, as is the nature of GAMs. This is the very problem we intended to solve by discussing NAMs - we want to be able to capture not only the relevance of input features, but of learnt concepts over those features.

Again, new model architectures have been introduced to resolve this. The aptly named Explainable Neural Network (xNN) [30] is an architecture which extends NAMs with a single linear "projection layer". These are equivalent to learning a GAM over *linear combinations* of input features. They are therefore fully described by the equations

$$\mathbf{a} = \mathbf{W}\mathbf{x} + \mathbf{b}$$

$$M(\mathbf{x}) = \sigma\left(\sum_i M_i(a_i)\right)$$

Where $\mathbf{W}, \mathbf{b}$ are learnable parameters as standard. We can interpret this model very similarly, by again plotting the univariate subnetworks M_i, and simply interpreting what a concept a_i represents by directly observing the linear combination. The UAT tells us that this single added layer is enough to model any function to an arbitrary precision, but in practice this hidden layer would need to be quite wide for anything other than the most trivial problems, and the features introduced in a large hidden layer may not be terribly intuitive to understand, and may even introduce a large bias.

We could extend this further, by adding more perceptron layers to capture more complicated relations between input features, but this naturally comes at the expense of interpretability. An ideal solution to this problem would allow for the model to be extended with more layers without sacrifice.

This motivates a new architecture for layers in our NN, as perceptron layers can be considered the main obstruction to interpreting our models.

Chapter 2

Logical Neural Networks

2.1 Introduction

We will discuss an NN architecture which attempts to learn boolean functions, instead of real functions. The restricted nature of boolean functions, and their use as a mathematical description of logic, allows a intuitive way of representating causation (e.g., if for some object x). The models that are created to solve such a problem are known as *Logical Neural Networks*[1] (LNNs)[2]. The subfield of ML concerned with learning solutions to logical problems with gradient-descent based methods is called *Neurosymbolic Machine Learning*.

The goal of the LNNs we discuss here will be to learn the optimal assignments for boolean variables within a statement described by the language of first order logic. This parallels the goal of MLPs to learn the optimal assignments for real variables within linear layers. LNNs achieve this through continuous optimisation using the standard approach of applying SGD methods with backpropagation.

It is interesting to note that the most widely researched approaches within the field of Artificial Intelligence (AI) until the 1990s were symbolic-based methods. There are many well studied algorithms that, given a set of logical predicates known to be true, attempt to capture the nature of the wider system in a single (ideally simple!) logical statement. These algorithms are known as Inductive Logic Programming (ILP) systems [18]. While very useful, they were found to be computationally intractible for more complex problems, notably those in Computer Vision and Natural Language Processing. Famously, Hubert Dreyfus predicted that symbolic methods were inherently incapable of fully capturing the complexity of such problems [8], stating that these relied primarily on unconscious processes rather than conscious symbolic manipulations. It seems most apt, therefore, to understand the rise of Deep Learning methods in the new millenium as reliant on capturing such "unconscious" processes.

The aim of neurosymbolic methods are thus to be able to capture the expressiveness of Deep Learning methods, without sacrificing the interpretability afforded by understanding the model in terms of symbolic manipulations. This is a difficult task!

2.2 Real Logic

We run into the important issue of $\{\mathbf{T}, \mathbf{F}\}$, the space of boolean values, not being continuous. One way of solving this issue is by extending the domain of possible logical assignments from $\{0, 1\}$, as above, to the closed interval $[0, 1]$. This is referred to as both *real logic*, (as in [26], [29], and much of the literature focusing on differentiable applications), and *fuzzy logic* (as in most foundational literature, namely [32], [17], [12]). Using the name "fuzzy logic" emphasises the importance of properties which are not relevant to the neurosymbolic architecture we will be discussing here, so we will not be using the term widely, but many of the following constructions are drawn from literature on fuzzy logic. We will discuss approaches in extending important logical operators (`OR`, `AND`, `NOT`, ...) to this new boolean space, and ways we may begin to use it to learn in an interpretable way.

[1] also *Neural Logic Networks, Logic Tensor Networks*
[2] also NLNs, LTNs

To fully define a "real logic", that is, an extension of classical logic to the space $[0,1]$, we want to define all the operators in a manner that, ideally, preserves many of the useful properties we see in the classical definition. At the very least, we want the values over the restricted domain $\{0,1\}$ to be the same as in classical logic.

It is well known that given a finite number of variables $\{x_i \mid i \in 1,\dots,N\}$, all boolean functions (that is, functions $\phi : \{\mathbf{T},\mathbf{F}\}^N \to \{\mathbf{T},\mathbf{F}\}$) can be expressed in terms of the operators $\neg$ and $\wedge$. Explicitly,

$$\begin{aligned}
a \vee b &= \neg(\neg a \wedge \neg b) \\
a \Rightarrow b &= \neg(a \wedge \neg b) \\
a \ \texttt{XOR}\ b &= \neg(a \wedge \neg b) \wedge \neg(\neg a \wedge b) \\
a \ \texttt{XNOR}\ b &= \neg(a \wedge b) \wedge \neg(\neg a \wedge \neg b) \\
\forall x, \phi(x) &= \phi(x_1) \wedge \cdots \wedge \phi(x_N) \\
\exists x, \phi(x) &= \neg(\neg\phi(x_1) \wedge \cdots \wedge \neg\phi(x_N))
\end{aligned}$$

If we can extend the operators $\wedge$ and $\neg$ to the full domain $[0,1]$, we can therefore do so for all the above operators also. For the remainder of this section, we will specify that $\mathbf{T} \coloneqq 1$, and $\mathbf{F} \coloneqq 0$, though there are alternative architectures where this is not the case [11].

2.2.1 Real Conjunction and Negation

We will take a set of properties that apply to classical conjunction $\wedge$ and require that the extension $\wedge : [0,1]^2 \to [0,1]$ has them also. The properties are;

$$\begin{aligned}
\text{(Associativity)}\ & (a \wedge b) \wedge c = a \wedge (b \wedge c) \\
\text{(Commutativity)}\ & a \wedge b = b \wedge a \\
\text{(Monotonicity)}\ & a \le b, c \le d \implies a \wedge c \le b \wedge d \\
\text{(Identity)}\ & \forall a \in [0,1], a \wedge 1 = a
\end{aligned}$$

The above are known as the *T-norm axioms* [16]. Note that they are a strict subset of the axioms required for $([0,1], \wedge, \vee)$ to be a boolean algebra, namely we are missing distributivity and idempotence. In fact, it is possible to construct a real logic that preserves these properties also, but there is precisely one such logic (known as the Minimum, or Gödel logic), and as we will see, it has flaws that make it less than ideal for gradient descent. The above axioms are, however, enough for $\wedge$ to have the correct output for the restricted domain $\{0,1\}$.

We can likewise define negation simply by $\neg : x \mapsto 1 - x$. In the fuzzy logic literature, this is known as *strong negation*, as there is an alternate formulation of negation that captures the intention of fuzzy logic more effectively.

It can be shown that the axioms as we have defined them allow for an infinite family of possible real logics. Some examples are given below;

Logic	$\forall$	$\exists$
Minimum	$\min\{x_1,\dots,x_N\}$	$\max\{x_1,\dots,x_N\}$
Product	$\prod_i x_i$	$1 - \prod_i (1 - x_i)$
Łukasiewicz	$\max\{\sum_i x_i - N + 1, 0\}$	$\min\{\sum_i x_i, 1\}$
Schweizer-Sklar	$\max\{\sum_i x_i^p - N + 1, 0\}^{\frac{1}{p}}$	$\min\{N - \sum_i (1 - x_i)^p, 1\}^{\frac{1}{p}}$
Yager	$\max\{1 - (\sum_i (1 - x_i)^p)^{\frac{1}{p}}, 0\}$	$\min\{(\sum_i x_i^p)^{\frac{1}{p}}, 1\}$

The examples are expressed as conjunctions of N variables, not just 2. p in the table above is a hyperparameter. Figures 2.1 shows more visually how some of these logics behave. Drastic logic, not listed in the table above, is 0 whenever 2 or more inputs are less than 1. Otherwise, it agrees with the other logics.

2.3 General Architectures

Now that we have explicit definitions for boolean-like algebras in the domain $[0,1]$, we can begin to formulate how we may learn in this setting.

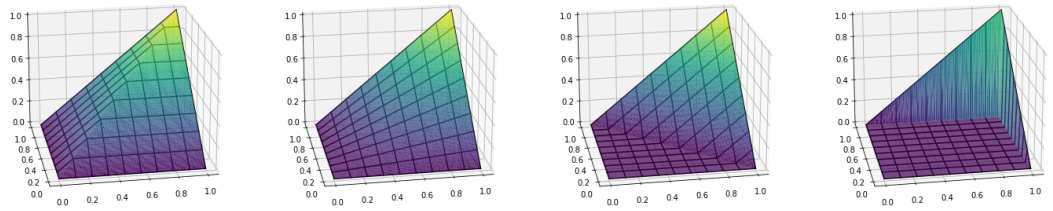

(a) Minimum (b) Product (c) Łukasiewicz (d) Drastic

Figure 2.1: Conjunction over various fuzzy logics. Note how pointwise gradients differ.

We first need to consider what problems we may want to solve. A basic problem is that of *satisfiability*, i.e., given a boolean function $\phi : \{0,1\}^K \to \{0,1\}$ which can be expressed in first-order logic, is there some element $\mathbf{x} \in \{0,1\}^K$ such that $\phi(\mathbf{x}) = 1$? If so, we want to find an example of said $\mathbf{x}$.

We can consider this as a continuous optimisation problem with $\mathbf{x}$ as a parameter. We can extend ϕ to the real domain $[0,1]$ by extending each operator in ϕ when expressed in the language of first-order logic. Then, by performing SGD as normal, we aim to minimise the loss function $\ell(\mathbf{x}) = \neg\phi(\mathbf{x})$.

To match the power of classical MLPs, we also want to be able to learn optimal *functions* ϕ. Suppose we have a dataset $\{(\mathbf{x}_i, y_i)\}_{i=1}^N$ where $\forall i, \phi(\mathbf{x}_i) = y_i$ for some formula $\phi : \{0,1\}^K \to \{0,1\}$ which need not have a known representation in classical first-order logic. Further suppose we have a function $\psi : \{0,1\}^{K+P} \to \{0,1\}$ expressed in first-order logic such that for some $\mathbf{w} \in \{0,1\}^P$, $\phi(\mathbf{x}) = \psi(\mathbf{x}, \mathbf{w})$. We consider $\mathbf{w}$ a parameter here, to be optimised. We could use a variety of losses - in the following we examine $\ell(\mathbf{x}, y; \mathbf{w}) = (y \texttt{ XOR } \psi(\mathbf{x}, \mathbf{w}))^a$, for some exponent $a \in [1, \infty)$ (as $\mathbb{E}_{\mathbf{x}}[\ell(\mathbf{x}, \phi(\mathbf{x}); \mathbf{w})] = 0 \iff \psi(\mathbf{x}, \mathbf{w}) = \phi(\mathbf{x})$), which we refer to as XOR loss, and binary cross-entropy, as is done in [27].

It is very feasible to find expressive enough ψ, as it can be shown that every boolean function ϕ can be expressed in a number of standard forms - Disjunctive Normal Form (DNF), and Conjunctive Normal Form (CNF), being two notable ones. To fit these two representations into the framework we have described, we need to be able to express how every variable x_i is represented in each normal form by appending appropriate parameter variables w_i.

In DNF, ϕ is expressed as a disjunction of conjunctions, with each conjunction described by a subset of input variables $\subseteq \{x_1, \ldots, x_K\}$, each variable being optionally "signed" (prepended with $\neg$). We can capture "membership" by boolean variables $m_{ij} \in \{0,1\}$, and signs by $s_{ij} \in \{0,1\}$. This allows us to represent a formula in DNF by

$$\begin{aligned} \phi(\mathbf{x}) &= \exists j,\ 1 \le j \le W,\ \phi_j(\mathbf{x}) \\ \text{where } \phi_j(\mathbf{x}) &= \forall i,\ m_{ij} \Rightarrow (x_i \texttt{ XOR } s_{ij}) \end{aligned}$$

for some assignment to the m_{ij}, s_{ij}. A similar form for CNF is,

$$\begin{aligned} \phi(\mathbf{x}) &= \forall j,\ 1 \le j \le W,\ \phi_j(\mathbf{x}) \\ \text{where } \phi_j(\mathbf{x}) &= \exists i,\ m_{ij} \wedge (x_i \texttt{ XOR } s_{ij}) \end{aligned}$$

In both cases, we can construct a function ψ with the m_{ij} and s_{ij} as parameters, and optimise over these parameters as above. Here $W \in \mathbb{N}$ is a hyperparameter which specifies the number of conjunctions (or disjunctions) in the function family ψ. Naturally, the larger W is, the more expressive ψ can be, and we know that $W = 2^K$ is enough to capture all possible functions ϕ. This very closely parallels the Universal Approximation Theorem (UAT) of MLPs with one hidden layer. It also very closely mirrors the concept of "reducing induction to satisfiability" seen in many ILP systems [9].

2.4 Analysis of a Toy Problem

The framework we have given is very general, and does not specify what real logic we are required to use. Indeed it does not even require that every operation need be from the same logic, only that they are correct on classical

boolean values $0, 1$. It is valuable, therefore, to compare each logic and analyse which logics are useful for which learning tasks.

In [29], the problem of satisfiability over $\phi(a, b, c) = (a \wedge b) \vee (c \wedge \neg a)$ is considered. We compare how the parameters a, b, c[3] evolve over each logic, given randomly initialised starting parameters.

Figure 2.2 show convergence of the output of ϕ for 1000 uniformly sampled random initialisations of the parameters a, b, c in the interval $(0, 1)$, using Adam optimisation [15] with a learning rate of 10^{-1}. Convergence to 1 represents finding a satisfying assignment, whereas anything else represents a failure to do so.

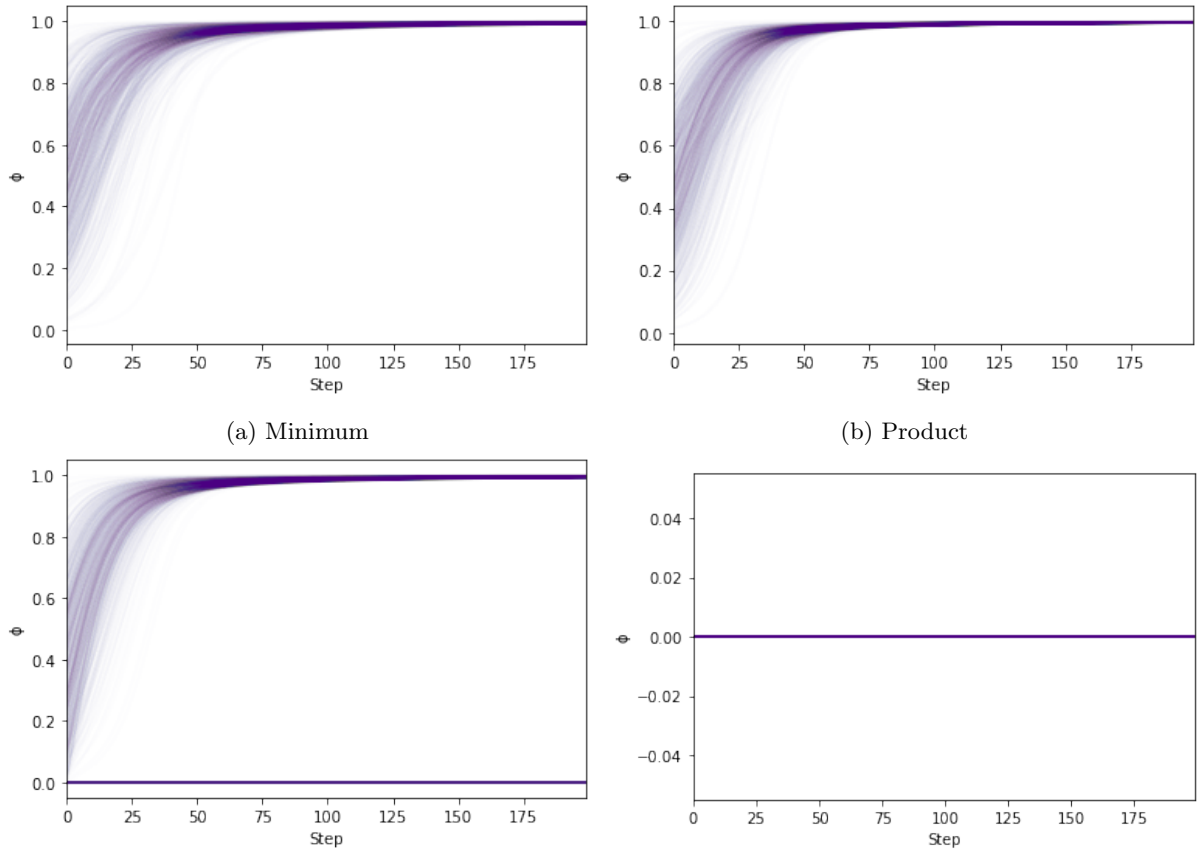

(a) Minimum

(b) Product

(c) Łukasiewicz

(d) Drastic

Figure 2.2: Convergence of toy problem $\phi(a, b, c) = (a \wedge b) \vee (c \wedge \neg a)$ for various fuzzy logics.

We see that the choice of logic has a profound impact on the convergence. Minimum and Product logic both reliably find a satisfying assignment of ϕ regardless of initialisation. Łukasiewicz logic finds a satisfying assignment in many instances, but very often fails to optimise at all. Drastic logic (somewhat obviously) never finds a satisfying assignment, regardless of initialisation.

2.4.1 Vanishing Gradients

The tests show that a majority of gradient samples for Łukasiewicz logic are precisely 0. By inspection of Figure 2.1c, we can see that there are large regions (i.e. regions of non-zero measure) where the function evaluates only to 0. It is natural that some observations would not allow us to make any meaningful inferences about the optimal values of each variable, especially in cases where the proportion of satisfying inputs is incredibly small. We observe however, that different choices of logic result in different proportions of vanishing gradient observations.

To explain this, we must discuss the nature of conjunction in each logic. In Łukasiewicz logic, for $a, b \in [0, 1]$ such that $a + b - 1 < 0$, the gradient of binary conjunction $\wedge$ is precisely 0. This means that a full $\frac{1}{2}$ of all possible input

[3]In practice, we actually consider satisfiability over parameters $a, b, c \in \mathbb{R}$ mapped into $[0, 1]$ with a sigmoid function, as we want to converge to parameters in the appropriate bounds.

arguments (uniformly distributed) give no meaningful inference. Aggregating over K variables, this generalises to a proportion of $1 - \frac{1}{K!}$ inputs having vanishing gradients, which is very obviously not ideal.

Therefore, in this framework, we prefer to use logics such that $\wedge$ has non-vanishing gradient almost everywhere - these logics are known as *strict*. Minimum and Product logics satisfy this condition, along with certain parameterisations of the Schweizer–Sklar and Yager logics.

2.5 Learning Functions

There are many well known algorithms for efficiently learning classical boolean functions $\phi : \{0,1\}^K \to \{0,1\}$ given prior knowledge of ϕ restricting it to a given family. Such algorithms often make logical inferences to determine the proper state of boolean parameters $\mathbf{w}$, with complexity guarantees that can be described within the Probably Approximately Correct (PAC) learning framework [14]. We propose equivalent algorithms in differentiable real logic, and hope for results as good, if not better, given an ideal optimisation regime.

Generalising these methods to real logic would have considerable benefits. For one, given gradient descent is by nature stochastic and (aside from current parameterisation) stateless, these methods would be inherently robust to noisy data and distribution shift in the learning dataset. A possible drawback is that correctness may only be guaranteed for data drawn similarly to the training dataset, introducing a potentially unavoidable bias.

2.5.1 Learning Conjunctions

The problem of learning conjunctions is a classical one in Computational Learning Theory (CLT). It is well known that determining conjunctions can be done PAC-efficiently [14] and is robust to noisy data [3]. The goal of this comparison, therefore, is simply to prove the viability of real logic for this application.

The classical algorithm relies on one important observation. Suppose ϕ is a conjunction, that is - it is a function of the form

$$\phi(x_1, \ldots, x_D) = y_1 \wedge \cdots \wedge y_N$$

for $y_i \in \{x_1, \ldots, x_D, \neg x_1, \ldots, \neg x_D\}$. If for some j, we have $\neg x_j$ but ϕ returns true, then x_j is not one of the terms y_i. Similarly $x_j \wedge \phi$ implies $\neg x_j$ is not one of the terms. If we begin with ϕ a conjunction over all possible such terms, and remove terms where possible, we are eventually left only with the terms actually present in the conjunction.

As discussed previously, we can model the same thing in real logic by introducing weight and sign parameters $\mathbf{m}$ and $\mathbf{s}$,

$$\psi(\mathbf{x}; \mathbf{m}, \mathbf{s}) = \forall i,\ 1 \leq i \leq D,\ m_i \Rightarrow (x_i \ \texttt{XOR} \ s_i)$$

and optimising $\mathbf{m}$ and $\mathbf{s}$. In the following, for initial simplicity, we set $\mathbf{s} = 0$ (i.e. we assume no signs $\neg$.)

We aim to learn conjunctions by randomly initialising values $\mathbf{m}$, before minimising for some loss function, such as those given in Section 2.3. Data pairs are generated by randomly sampling bits $\{0,1\}^D$, and mapping them through a predefined goal conjunction with N terms. We vary many aspects of this model, including conjunction size D, number of present terms N, choice of real logic, optimiser, learning rate and loss exponent a.

Some results using this architecture are not promising. Figure 2.3 shows convergence of the average distance of a parameter from it's optimal (i.e. correct) value, with the `XOR` loss $\ell(\mathbf{x}, y; \mathbf{w}) = (\psi(\mathbf{x}; \mathbf{w}) \ \texttt{XOR} \ y)^a$ using an Adam optimiser with a learning rate of 10^{-2}, when learning unsigned conjunctions in the Product logic. Each test is run several times, with the convergence of each run plotted on the graph. Both training and test data are uniformly sampled random bits $\{0,1\}^D$, with each epoch representing 10,000 such samples. We see that for low dimensionality, convergence is quite fast, whereas minimal changes occur with dimensionality any higher than 100. This is of course an issue.

We see better results when using binary cross-entropy. Figure 2.4 displays the results from the same test, with differing loss function. We see that dimensionality $D = 100$ now can be learnt, but we still cannot go much higher.

2.5.2 Vanishing Gradients in Strict Logics

To determine why this happens, we need only observe the induced gradient of the network. It is well known that a large family of T-norms can be constructed using what is known as an *additive generator*, that is, a function

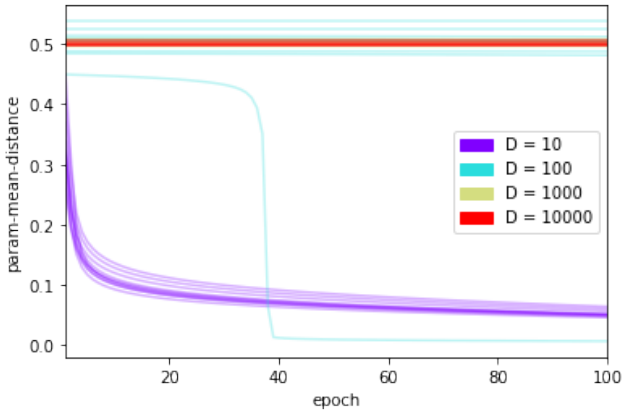

(a) 1-term conjunction

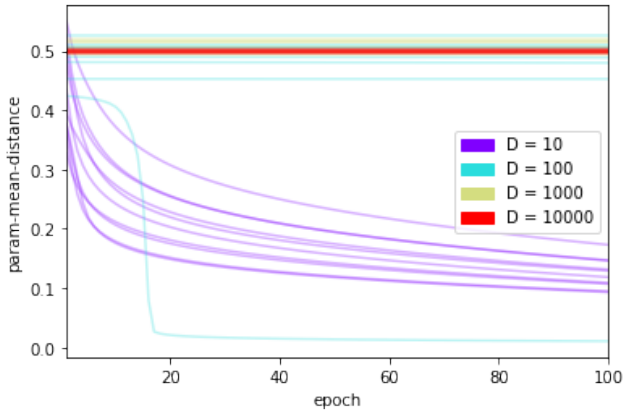

(b) 5-term conjunction

Figure 2.3: Convergence of mean distance from optimal parameters when learning conjunctions in the Product logic. Each test is run 10 times, with `XOR` loss, using exponent $a = 10$.

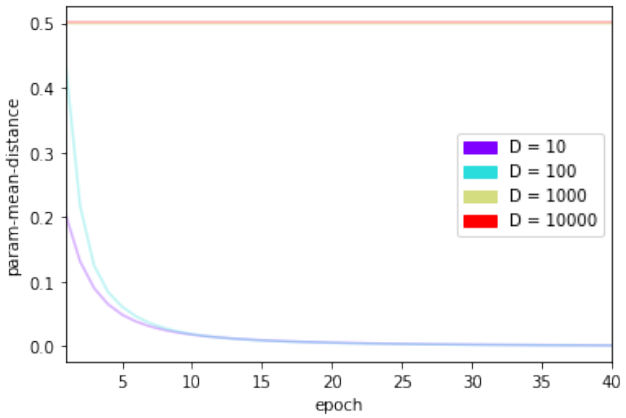

(a) 1-term conjunction

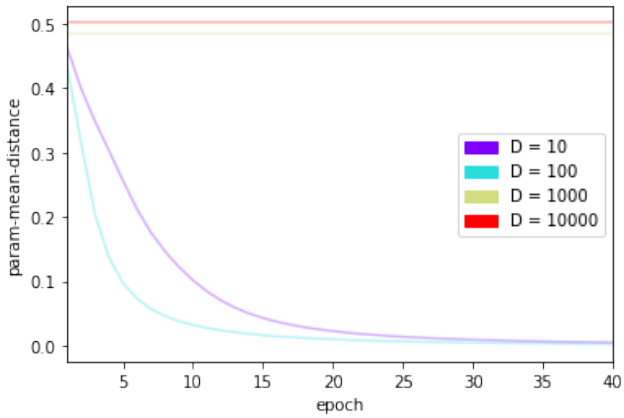

(b) 5-term conjunction

Figure 2.4: Convergence of mean distance from optimal parameters when learning conjunctions in the Product logic, with exponent binary cross-entropy loss.

$f : [0, 1] \to \mathbb{R}$ associated with a given logic, such that $a \wedge b = f^{-1}(\min\{f(a) + f(b), f(0)\})$. This definition allows us to also say $\forall i, x_i = f^{-1}(\min\{\sum_i f(x_i), f(0)\})$. Some additive generators have $f(x) \to \infty$ as $x \to 0$, and in these cases $a \wedge b = f^{-1}(f(a) + f(b))$ for $a, b \neq 0$.

Suppose $\sum_i f(x_i) \leq f(0)$ (which is trivially satisfied if $\lim_{x\to 0} f(x) = \infty$). Then;

$$\begin{aligned} \forall i, x_i &= f^{-1}(\sum_i f(x_i)), \text{ so} \\ \frac{\partial}{\partial x_j} \forall i, x_i &= \frac{f'(x_j)}{f'(f^{-1}(\sum_i f(x_i)))} \\ &= \frac{f'(x_j)}{f'(\forall i, x_i)} \end{aligned}$$

Some examples of additive generators, as well as explicit values for the derivative above, are given in the following table. Note that if $\sum_i f(x_i) > f(0)$, all gradients are vanishing.

Logic	$f(x)$	$\frac{\partial}{\partial x_j}\forall i, x_i$
Product	$-\log x$	$\prod_{i\neq j} x_i$
Łukasiewicz	$1-x$	1
Schweizer-Sklar	$\frac{1-x^p}{p}$	$\left(\frac{x_j}{\forall i, x_i}\right)^{p-1}$
Yager	$(1-x)^p$	$\left(\frac{1-x_j}{1-\forall i, x_i}\right)^{p-1}$

The Minimum logic has no additive generator. From the table, the influence of dimensionality now becomes apparent.

Suppose each aggregate conjunction $\forall i, x_i$ is over D variables. In the product logic, if the x_i are independently uniformly distributed in $[0,1]$, $\mathbb{E}\left[\frac{\partial}{\partial x_j}\forall i, x_i\right] = \mathbb{E}\left[\prod_{i\neq j} x_i\right] = 2^{D-1}$. Thus the total derivative $\nabla_\forall$ has expected magnitude $\mathbb{E}\left[\|\nabla_\forall\|_2\right] \leq \mathbb{E}\left[\sum_j \frac{\partial}{\partial x_j}\forall i, x_i\right] = D2^{D-1}$. With high dimensionality D, the gradients quickly degrade.

Other T-norms do not suffer this same issue. For example, Łukasiewicz logic has a gradient of 1 in every dimension when the function is non-vanishing, however we have shown previously in Section 2.4.1 that the proportion of vanishing inputs is it's own curse of dimensionality, as it is not strict. Minimum logic has constant $\|\nabla_\forall\|_2 = 1$, however we will see later that there are still issues with optimisation. In Appendix **??**, we show that for Schweizer-Sklar logic with parameter p, the magnitude of $\nabla_\forall$ is lower bounded by $D^{\frac{1}{p}-\frac{1}{2}}$. In this section, we use $p=-2$, thus making the lower bound $D^{-1} \leq \|\nabla_\forall\|_2$, which is a vast improvement on an upper bound of $D2^{-D}$ seen in the Product logic. Empirical confirmations are given in Figures **??** and **??** in the Appendix.

This can also explain why binary cross-entropy performs better than `XOR` loss in this domain. With this loss, outputs are mapped through a log function. If we consider the Product logic, this is equivalent to interpreting conjunctions as a log summation $\sum_i \log x_i$, which means the values of each variable no longer affect each other's gradients, which would help remedy one cause of the curse of dimensionality.

2.5.3 Architectural Improvements

To fix the problem described in the previous section, in [29], the authors propose a method whereby only a subset of dimensions are conjoined during training passes. Fixing the size of this subset to a number less than 100 should allow for the mitigation of any dimensionality effects on convergence, as we are only optimising this subset of parameters at any one time. This does result in a biased gradient estimator, as we are ignoring many inputs, but in practice this shows to broaden the space of problems that can be solved using this method. This optimisation can be seen as analogous to the common "dropout" method in traditional neural networks, used to reduce overfitting during training [13].

We will refer to this method as the *subset optimisation*. Results for conjoining only 50 inputs at a time, chosen at random, are shown in Figure 2.5. We see that this extends the viability of this method to much larger dimensionalities than was previously possible, even when using the Product logic, which we know to not be ideal.

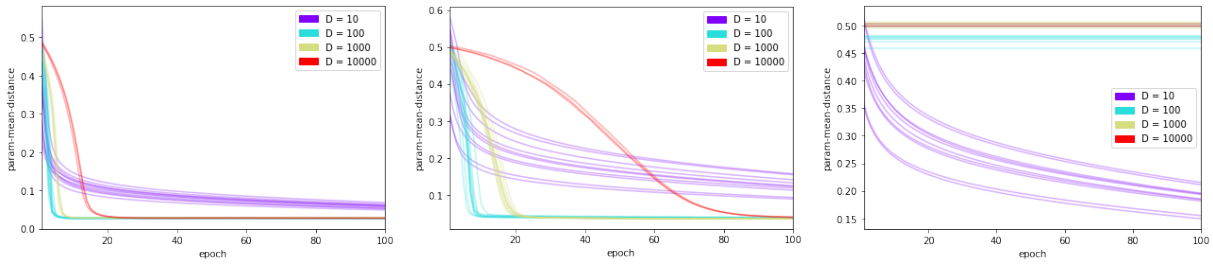

(a) 1-term conjunction (b) 5-term conjunction (c) 20-term conjunction

Figure 2.5: Convergence of mean distance from optimal parameters when learning conjunctions in the Product logic, with the size-50 subset optimisation, under `XOR` loss with exponent $a = 10$.

2.5.4 Class Imbalance and Parameter Crispness

In Figure 2.5, we notably see that, whilst applying the subset optimisation makes scaling the dimension of a conjunction viable, what is not viable is increasing the size of the number of terms in the conjunction. If a boolean function is a conjunction of N terms, only a fraction of 2^{-N} of all possible inputs will be satisfying. Thus, our learning becomes exponentially worse with increasing N. This problem is referred to as class imbalance.

We can explicitly sample the gradients to see how this manifests more directly. Suppose we have a proposed conjunction $\phi(\mathbf{x}) = x_1 \wedge x_2 \wedge x_3$, but we learn that $x_1 = \mathbf{F}$ while $\phi = \mathbf{T}$, for some training data point. If ϕ were as we assumed, ϕ would be $\mathbf{F}$ in this case, but it is not. Thus x_1 cannot be one of the terms in ϕ. Applying this more generally is what is used in classical algorithms for learning conjunctions given noise-free data [14].

We would expect to see a similar effect in the gradient estimator that we derive through backpropagation. To test for this, we uniformly sample random initialisations of a real conjunction model, and observe the gradient estimations that result from an entire epoch of training inputs. Figure 2.6 displays the results of this procedure. A conjunction over $D = 10$ variables containing $N = 4$ present terms was used to best convey the issue in the empiric results.

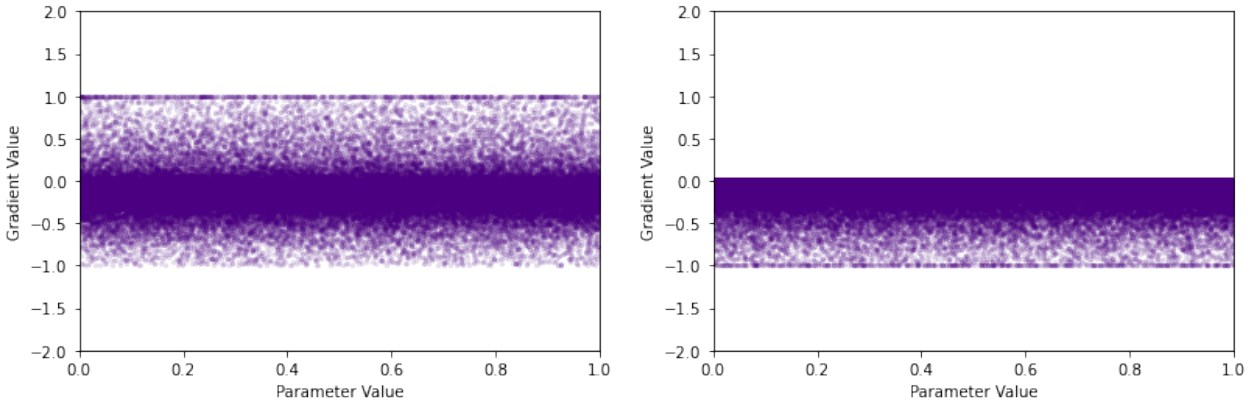

(a) Gradient samples for correct parameter $\mathbf{F}$

(b) Gradient samples for correct parameter $\mathbf{T}$

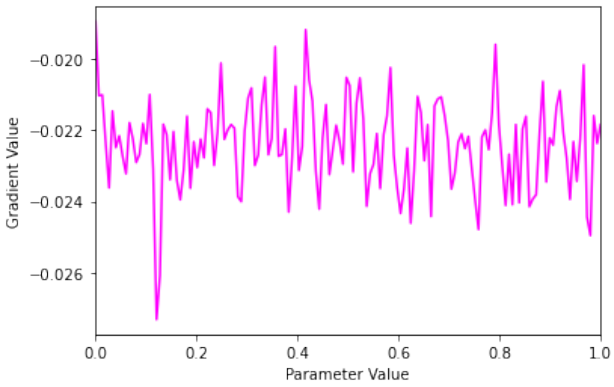

(c) Mean gradient estimator for correct parameter $\mathbf{F}$

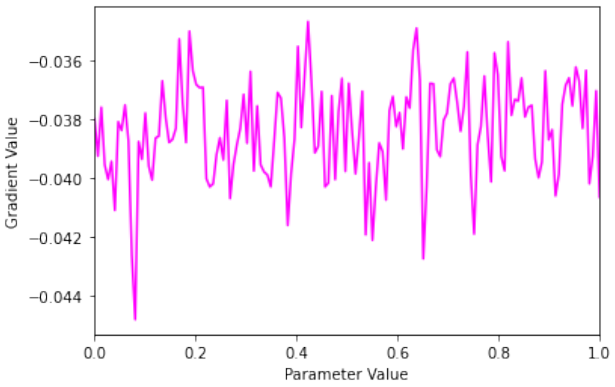

(d) Mean gradient estimator for correct parameter $\mathbf{T}$

Figure 2.6: Gradient estimations over the problem of real conjunctions under `XOR` loss with exponent $a = 1$.

We do see that the gradient estimator behaves differently depending on the true valuation of a given logical parameter. If the true value is $\mathbf{F}$, any input sample with a correct output of $\mathbf{T}$ results in a positive gradient estimation, thus decreasing the parameter on the next optimisation step, as can be seen in Figure 2.6a. This is exactly the kind of behaviour we would expect, and it represents a faithful translation of logical inference to the real domain. Whenever the output is $\mathbf{F}$, the model increases all parameters, as no meaningful inference can be made, which can be seen in both Figures 2.6a and 2.6b. This can be interpreted as the model aiming to be robust to noisy data.

The samples above show that it is impossible for terms which are indeed part of the true conjunction to not be

represented in the learnt model, as their parameterisations can only increase. The mean gradient estimator in Figure 2.6d reflects this, as it is firmly below 0 no matter the parameterisation. If the term is not in the true conjunction, however, Figure 2.6c shows that we unfortunately see that the gradient estimator is still negative, meaning the term appears in the learnt conjunction, regardless of initial parameterisation.

This is the result of the class imbalance problem. Despite the gradients being in the right direction at every step, the overall result is inaccurate, because inferences are not being well capitalised if they cannot be frequently made.

What is interesting is that increasing the value of the exponent a appears to resolve this issue. In all our successful tests, we use a value of $a = 10$. A plot of gradient samples can be found in Appendix **??**. We see that as the exponent increases, the direction of the gradients become more accurate, and the magnitude of the gradients become larger for significantly incorrect values. However, for parameter values that are near to 0.5, no significant gradient is observed. Values 0 and 1 are referred to as "crisp" boolean values, so one could interpret this as the regime failing to "crispen" values effectively, despite correctly signed gradients. Appendix **??** contains further examples of how this loss fails due to the curse of dimensionality - in all the plots in this section, we use dimensionality $D = 10$, but for $D = 100$ the gradients quickly vanish.

A significant observation therefore, which was eluded to Section 2.5.2, is that binary cross-entropy, with appropriate choice of logic, suffers none of these problems.

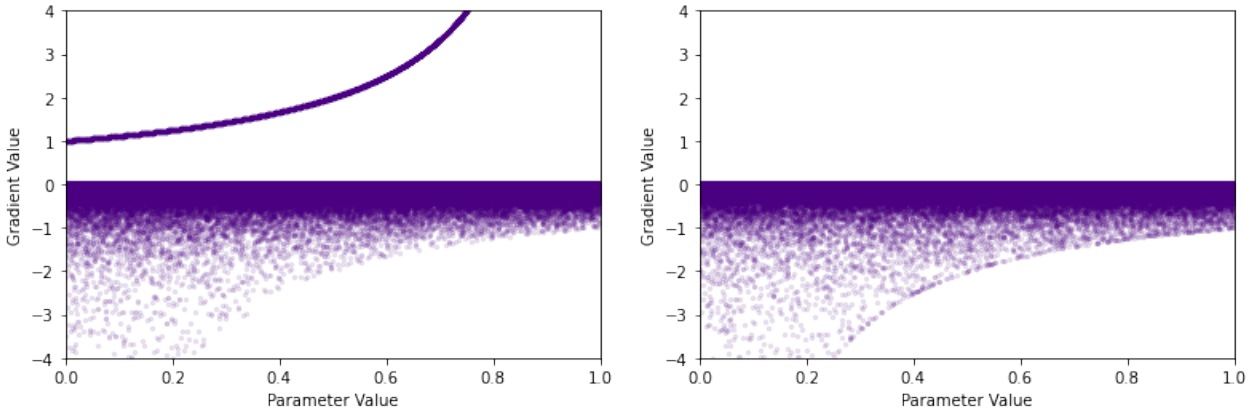

(a) Gradient samples for correct parameter **F**

(b) Gradient samples for correct parameter **T**

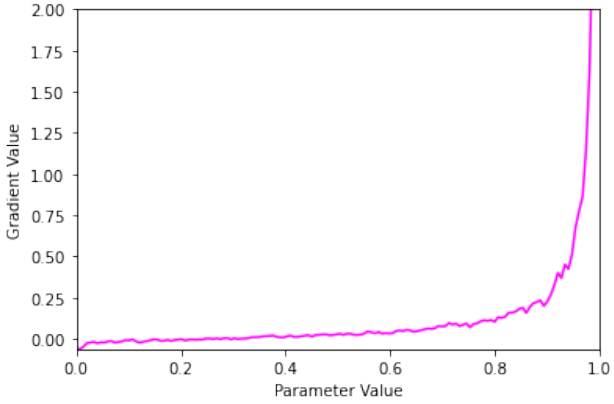

(c) Mean gradient estimator for correct parameter **F**

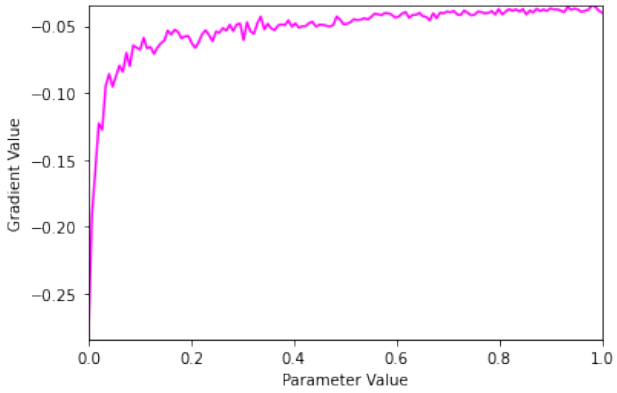

(d) Mean gradient estimator for correct parameter **T**

Figure 2.7: Gradient estimations over the problem of real conjunctions under binary cross-entropy loss.

Figure 2.7 shows how binary-cross entropy loss not only has a gradient estimator with correct direction, but also of greater magnitude, regardless of current parameterisation. Later empirical results will show that this does have a profound effect on convergence.

We have demonstrated that varying our choice of loss has a significant effect on not only the rate of convergence, but the correctness of the gradient estimator as well. Appendix **??** contains more such examples, that show how

varying the logic, dimension and choice of loss function have an effect on the gradient estimator.

2.5.5 Empiric Comparison of Logics

We have discussed what effect varying the choice of logic has on the gradient estimator $\nabla_\forall$, but we have not seen what effect this directly has on convergence. Figure 2.8 shows that this effect is profound. Here, a "correct" parameter is one which is within 0.5 of it's optimal value.

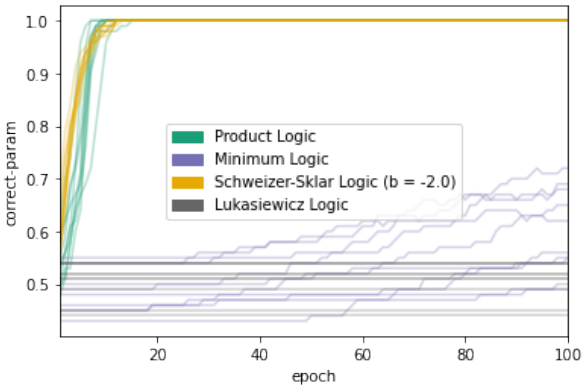

(a) Proportion of correct parameters for $D = 100$

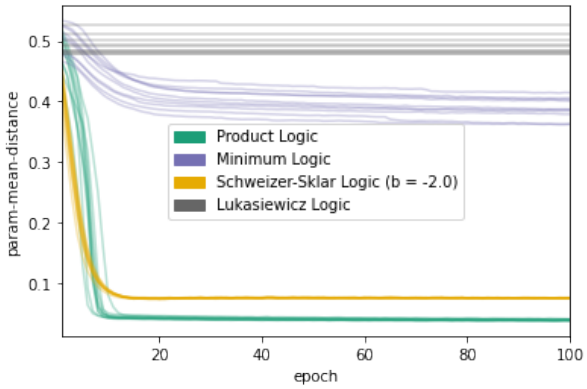

(b) Mean distance of parameters from optimum for $D = 100$

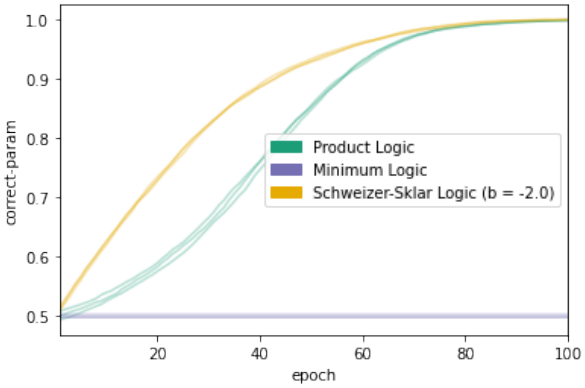

(c) Proportion of correct parameters for $D = 10000$

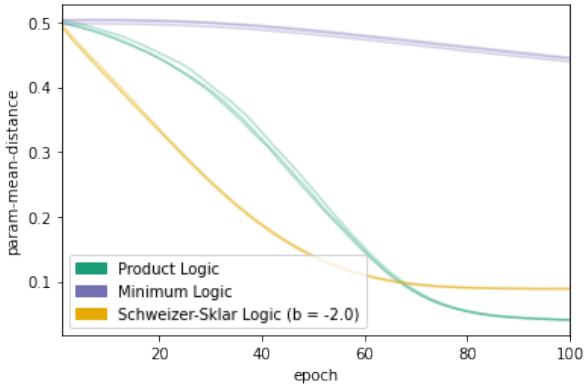

(d) Mean distance of parameters from optimum for $D = 10000$

Figure 2.8: Convergence over various logics under `XOR` loss $a = 10$. $N = 5$ terms, subset optimisation.

The plots show that, as in Figure 2.2, Lukasiewicz logic fails even with the discussed optimisations.

Minimum logic is not far behind - while Figure 2.8a shows the proportion of correct parameters increasing gradually for $D = 100$, this proportion does not improve whatsoever for $D = 10000$. This may be due to the fact that in Minimum logic, only one input variable to a conjunction has non-zero gradient at a time, as can be seen in Figure 2.1a. This restriction does not allow the optimisation regime to traverse the parameter space in an efficient manner. [29] refers to this problem as the *binarization* of gradients. Empirical examples of this binarization can be found in Appendix **??**.

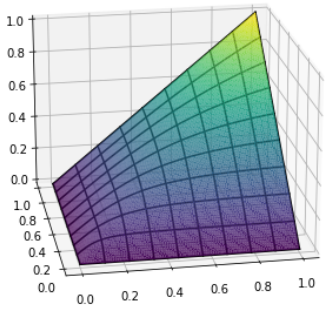

Figure 2.9: Schweizer-Sklar T-norm ($b = -2$)

We have already mentioned in Section 2.5.2 that Product logic suffers it's own curse of dimensionality, and we can see this in how it initially has poor convergence in Figure 2.8c. However, as parameters are optimised, the all inputs to the conjunction approach 1, and thus the gradients increase in value. This results in a quickening in convergence

rate around 40 epochs, before finally plateauing.

We also see the Schweizer-Sklar logic performs very efficiently, as the bounds derived in Appendix **??** predict. What is interesting to note is that, for $p = 0$, Schweizer-Sklar logic is precisely the Product logic, and for $p = -\infty$, it is precisely the Minimum logic. We can therefore also interpret Schweizer-Sklar (with a parameter $p = -2$ as used in the tests) as being a "middle ground" between the two logics, having a guaranteed significant gradient without suffering from binarization.

Of note is that, as we can see in Figure 2.8d, Product logic still outperforms Schweizer-Sklar logic in the "crispness" of it's learnt real parameters, as the former converges to an average distance considerably lower than that of the latter. Under binary cross-entropy loss, we see an interesting result.

Figure 2.10 shows the result of training under binary cross-entropy loss, both with and without the subset optimisation. The subset optimisation continues to work with the Product logic, albeit not as well. It however has a disasterous effect on Schweizer-Sklar logic, which not only fails to converge to optimal values, but goes in the wrong direction.

This is not observed without the subset optimisation. As we'd expect, the curse of dimensionality results in the Product logic implementation failing to converge at all. The Schweizer-Sklar implementation performs spectacularly well. It is significantly more efficient than under `XOR` loss - under `XOR` loss, with a dimensionality $D = 10000$, it takes roughly 40 epochs to achieve parameter correctness greater than 90%. Under binary cross-entropy loss, it only takes around 5. It further improves in the crispness of it's learnt parameters. In Figure 2.8, we saw that every logic failed to achieve optimal (i.e. close to 0) distance from optimal parameters. Under this regime, however, we can achieve this.

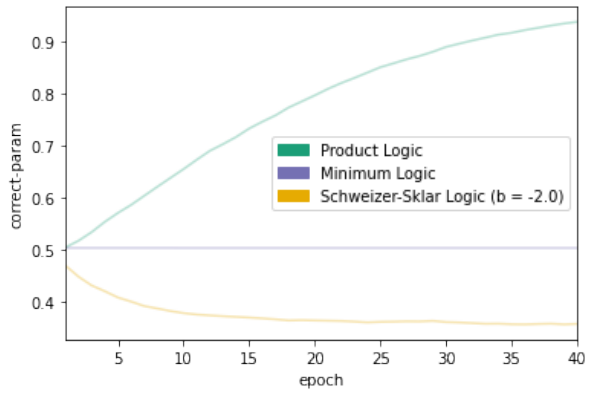

(a) Proportion of correct parameters with subset optimisation.

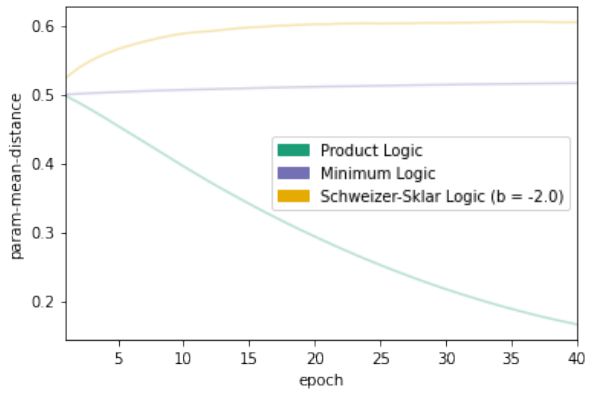

(b) Mean distance of parameters from optimum with subset optimisation.

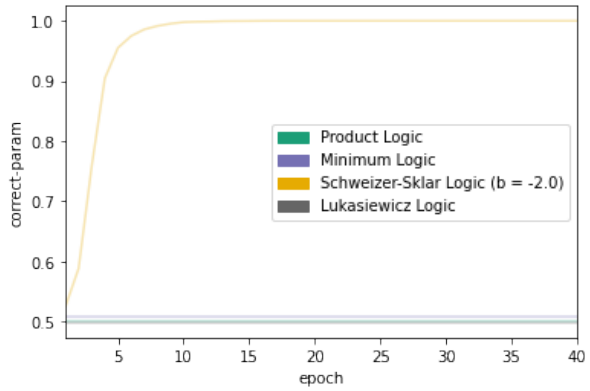

(c) Proportion of correct parameters without subset optimisation.

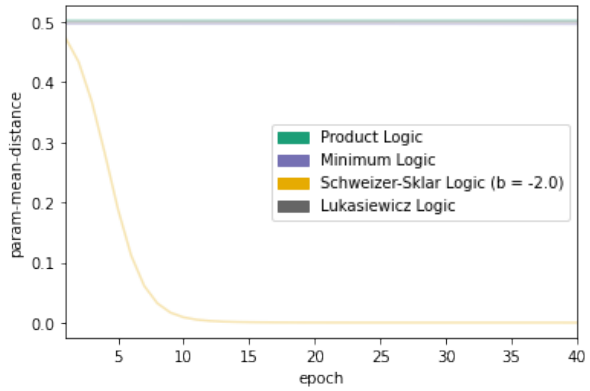

(d) Mean distance of parameters from optimum without subset optimisation.

Figure 2.10: Convergence over various logics under binary cross-entropy loss, $N = 5$ terms, $D = 10000$ dimensionality.

2.5.6 Suboptimal Predictions

Crispness is important if we wish to use any of these models to actually predict outputs. Suppose that we have correct parameterisations for every term, but with a distance of 0.25 from crisp values $0, 1$. In product logic, $0.25 \Rightarrow 0 = 0.75$, whereas in classical logic this would round to $\mathbf{F} \Rightarrow \mathbf{F} = \mathbf{T}$. taking the product over a number of such terms that increases linearly with N gives us an upper bound of $O(0.75^N)$ for the actual output. Since randomly sampled input bits generally have a proportion of bits with value 0 close to $\frac{N}{2}$, most outputs are guaranteed to be near 0. While many regimes can guarantee 100% of parameters are "correct", the nature of fuzzy logic means the output isn't necessarily translated into correct outputs.

Figure 2.11 shows the convergence of the proportion of corrects outputs under various regimes. Of note is that, for $N \geq 100$ under Product logic, the proportion of correct outputs does not meaningfully differ through optimisation. The stagnant proportion is also somewhat around $1 - 2^{-5} \approx 0.968$, which suggests that the output only ever evaluates to false, as this 2^{-5} represents the proportion of true outputs for conjunctions of 5 terms.

This is not surprising, as we have just discussed how this model poorly approximates the true crisp parameterisations $0, 1$, which would result in the output degrading to 0, even if the parameters are all correct.

However, as we have discussed, Schweizer-Sklar logic can approximate crisp values, and does not suffer the curse of dimensionality (as much). This can be observed in Figure 2.11c. In fact, convergence seems to suffer only linearly in $\log D$.

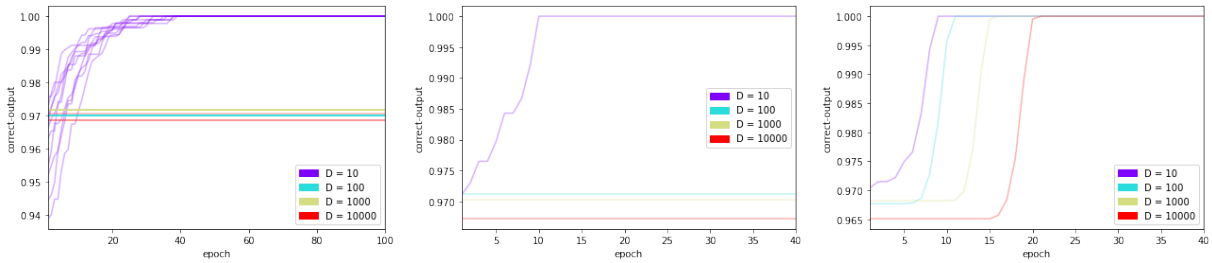

(a) Product logic, subset optimisation, XOR, $a = 10$ loss.

(b) Product logic, subset optimisation, binary cross-entropy loss.

(c) Schweizer-Sklar logic $p = -2$, no subset optimisation, binary cross-entropy loss.

Figure 2.11: Convergence of proportion of correct outputs, $N = 5$ terms.

2.5.7 Conclusions

In learning conjunctions, we have experimented with a variety of logics, loss functions, and additional optimisations to find solutions to the many issues experienced in relaxing classical logic to the real domain. Class imbalance results in inaccurate gradient estimators, while the curse of dimensionality results in vanishing ones. Many logics have gradient estimators which are precisely 0 in a non-negligible region of the parameter space. Even in logics where this isn't the case, for example the Minimum logic, we still suffer due to the gradients being *binarized*, we can only optimise one input at a time. Finally, the lack of crispness in our learnt parameters prevents the predicted outputs from being accurate.

If we learn this problem using Schweizer-Sklar logic under a binary cross-entropy loss, we can resolve all these issues to a satisfactory level. Formal lower bounds exist on the magnitude of the gradient estimator for increasing dimensionality, and class imbalance does not as significantly effect the correctness of the gradient direction under this loss. We can now experiment with more complicated problems.

2.6 Learning Arbitrary Functions

An important result from CLT is that with the assumption that RP $\neq$ NP, it can be shown that learning boolean functions in DNF is not PAC-efficient *in general* [14]. Hopefully, relaxing boolean constraints from the discrete to the real domain would allow us to overcome this issue.

Add test results here

Add analysis

It is important to note that

- Suddenly not convex (much like MLP) - Suffers greatly

2.7 Alternative Frameworks

The toy problems above show that the framework we have introduced is not adept at learning boolean functions in general. The appeal instead is that it is simple, and *extensible*. A neurosymbolic layer as we have described can be embedded within a larger model, that may also contain traditional perceptron layers. These mixed models could lend their correctness to traditional NN theory, and their interpretability to their neurosymbolic aspect. In this section, we will discuss other existing neurosymbolic methods, and judge them based on the possibility of use in this application.

One common feature of many of the architectures we have not yet discussed is that logical variables $\mathbf{x}$ explicitly describe some parent object. In the language of our real logic architecture, there exists some universe of objects O such that boolean inputs to ϕ describe an object $o \in O$ in the form of a *unary atom*, e.g. $\text{isGreen}(o), \text{isBig}(o)$. The output of ϕ can be interpreted as the valuation of a further unary predicate. Learning ϕ is equivalent to learning some "if and only if" relationship between different properties of the object $o \in O$, if such a relationship exists.

2.7.1 Alternative Applications of Real Logic

As mentioned previously, classical symbolic approaches to AI research involve the use of ILP systems. A formal description of an ILP system is one which can solve problems of the following form. Given some background knowledge B of the world of objects O in the form of a logical statement, and new observations of *positive and negative examples* E^+ and E^-, expressed as conjunctions of *ground literals* (e.g. $\text{isGreen}(o), \neg\text{areFriends}(a, b)$), we aim to find some hypothesis statement h such that $B \wedge h$ satisfies all new observations. Formally, we require *sufficiency* $B \wedge h \vDash E^+$, and *consistency* $B \wedge h \wedge E^- \nvDash \mathbf{F}$ of the constructed h.

Our current real logic framework solves a real relaxation of the ILP problem where E^+ and E^- are all instances of the same unary predicate. There exist differentiable real logic solvers for general ILP problems [9], [22]. Such implementations improve on classical ILP methods as they are robust to noisy data while still being adept at pattern finding.

Other implementations relax real logic further by removing the requirement for all T-norm axioms to be satisfied. [25] introduces *Weighted Non-Linear Logic*, which is conceptually similar to Łukasiewicz logic with the addition of a bias parameter β which is also optimised during learning. The source paper promotes this reformulation as it removes constraints from the problem of optimisation, though the algorithm introduced in the paper as stated cannot be embedded into a mixed model.

2.7.2 Embedded Logic and Relations

Many developments is neurosymbolic learning involve embedding objects into n-dimensional real vector spaces to exploit properties of this space. Word2vec [19] is a model for learning optimal embeddings of natural language atoms in a high-dimensional vector space. Such embeddings were found to preserve relationships between words through vector arithmetic [20] (e.g. Father $-$ Man $+$ Woman $\approx$ Mother). This can be interpreted as a (relaxed) ILP system which learns over the space of *binary* atoms. Learning embeddings of objects $o \in O$ in this manner will aid in extending our current real logic model to mixed models.

In [26], the notion of a *grounding* is introduced - before applying any real logic operators, objects $o \in O$ are mapped into $\mathbb{R}^n$ through some canonical function $\mathcal{G} : O \to \mathbb{R}^n$. An m-ary predicate P is then interpreted as a function

$\mathbb{R}^{n\times m} \to [0,1]$. The value of $\mathcal{G}$ may then be learnt in a manner which best evaluates predicates P for elements of the test dataset.

Further, [11] suggests that not only should objects be embedded into a real vector space, but that boolean values should be as well. In this system, boolean values are encoded over an n-dimensional unit sphere S_{n-1}, and logical operators are required to map the encodings of $\mathbf{T}$ and $\mathbf{F}$ appropriately in this space. Introducing new dimensions may aid in improving model quality, without sacrificing interpretability as activations can be collapsed back into "real logic" through a similarity metric $\textsc{Sim} : S^2_{n-1} \to [0,1]$. Cosine similarity (which corresponds to minimum distance travelling along the unit sphere) is generally used. [27] improves upon this by also learning core operators $\wedge, \vee, \neg$ as DNNs, with correctness ensured through regularisation rather than the architecture itself. This model has been used to develop high quality collaborative filtering algorithms [6].

2.7.3 Bayesian Models and Probabilistic Logic

Another approach which could be considered a continuous relaxation of classical logic is in modelling boolean values as distributions over deterministic values $\{\mathbf{T}, \mathbf{F}\}$. Bayesian methods are well studied for this application, with many efficient methods existing for learning the distributions of random variables expressed in terms of a random field. Probabilistic programming languages [10] are able to describe such problems over Bayesian Networks in an highly interpretable manner. Learning probability distributions over the parameter space $\mathbf{w}$ may prove a more interpretable solution, and further may solve some of the convergence issues seen due to many problems being non-convex. If we interpret real booleans $[0,1]$ as parameters of a Bernoulli distribution over values $\{\mathbf{T}, \mathbf{F}\}$, we can analogize real logic models using the product logic to modelling a random field such that all parameters $\mathbf{w}$ are independent of each other. In this interpretation, we see that using general Bayesian models increases the expressivity of our model by introducing dependencies between parameters $\mathbf{w}$. Arbitrary dependencies can be modelled using Normalizing Flows [23].

Bayesian methods are very general, and many approaches exist which are specialised for uses in logic. Bayesian networks are restrictive as they model variable dependencies as a Directed Acyclic Graph (DAG), whereas many dependencies in logic are cyclic (most notably the relation $\iff$). Markov Networks describe dependencies between random variables as edges in a graph, meaning that any two variables that are not adjacent are conditionally independent. These are used to capture logical inferences in the popular Markov Logic Network (MLN) model [24], which corresponds logical atoms to vertices, and formulae to cliques in the graph. Probabilistic Soft Logic [4] further develops on this by introducing a PPL to describe instances of a model similar to MLNs, which can be used to better interpret the results of learning using such methods.

Chapter 3

Application to Complex Problems

We have seen how our architecture is adept at learning problems in the form of boolean functions. There are many problems, however, that cannot be easily modelled by such functions. This chapter will focus on applying the methods we have discussed to problems in image classification. Using the classical example of MNIST [7], an input image representing a handwritten digit from 0 to 9 is mapped to a probability distribution over all possible classifications. Deep learning proved to be very effective at this task [7]. We hope to build an architecture that would be reasonably effective, while incorporating neurosymbolic elements that would allow us to interpret the learnt model.

3.1 Architecture

In Section 2, we discussed how the use of binary cross-entropy loss, as opposed to other loss functions, makes many boolean problems tractably learnable under the proposed architecture. The same reasoning applies to other forms of cross-entropy. If we have a well-trained MLP model for MNIST classification, and we aim to train a neurosymbolic model for the same problem, we can take the cross-entropy between the output distributions of the two models as an effective loss function.

We therefore construct an architecture as follows. Suppose we have dataset of pairs $[0,1]^D \times [0,1]^M$. Let m, ψ represent models (with implicit parameters) $[0,1]^D \to [0,1]^M$, with m being a traditional MLP model, and ψ a neurosymbolic model. Define the *difference loss* ℓ_d to be the cross entropy of the neurosymbolic model with respect to the MLP model, that is;

$$\ell_d(\mathbf{x}) = \sum_{i=1}^{M} p_m(i) \cdot \log p_\psi(i)$$

Where p_m is the vector $\text{softmax} \circ m(\mathbf{x})$ for input $\mathbf{x} \in [0,1]^D$, and p_ψ is the same for ψ. Our overall loss function would then take the form

$$\ell(\mathbf{x}, y) = \sum_{i=1}^{M} \left[\mathbb{1}(y = i) \cdot \log p_m(i)\right] + \delta \ell_d(\mathbf{x})$$

for some hyperparameter $\delta > 0$. The first term is the traditional multi-class cross-entropy used to train any classification model, while the second term is the difference loss we have already discussed.

In MNIST, images are grids of size 28×28, making for $D = 784$. Too many parameters would make our model more difficult to interpret, but by chaining the joint model multiple times, we can overcome this. Suppose we had pairs of models $(m_1, \psi_1), \ldots, (m_n, \psi_n)$ defined similarly to before. A more general loss would then be defined by

$$\begin{aligned} \mathbf{z}_0 &= \mathbf{x} \\ \mathbf{z}_i &= m_i(\mathbf{z}_{i-1}) \text{ for all } i = 1, \ldots, n \\ \ell(\mathbf{x}, y) &= \sum_i \left[\mathbb{1}(y = i) \cdot \log \text{softmax}(\mathbf{z}_n)(i)\right] + \delta \sum_{i=1}^{n} \ell_{d,i}(\mathbf{z}_{i-1}) \end{aligned}$$

where $\ell_{d,i}$ is the difference loss for the ith model pair (m_i, ψ_i). The model we actually use has $n = 2$ pairs of models. m_1 has no hidden layers, and has output dimension 128. m_2 has one hidden layer of size 64, before outputting values of size $M = 10$. Every MLP model ends in a softmax function so that outputs are in the interval $[0, 1]$, but for the remaining non-linearities, we use the "LeakyReLU" activation function [31]. We also replace the difference loss $\ell_{d,1}$ for the first pair with ℓ_2 hinge loss on the MLP model m_1's parameters;

$$\ell(\mathbf{x}, y) = \sum_i \left[\mathbb{1}(y = i) \cdot \log \operatorname{softmax}(\mathbf{z}_n)(i)\right] + \delta\ell_{d,2}(\mathbf{z}_1) + \lambda\ell_2(m_1)$$

where $\lambda > 0$ is another hyperparameter. This is done as m_1 is simply a generalised linear model, which is less difficult to interpret, as long as the model does not overfit to random noise, which we control using ℓ_2 regularisation.

The neurosymbolic model ψ_2 is a series of $M = 10$ DNF models under Schweizer-Sklar $p = -2$ logic, as described in Section 2.6. Each DNF model is the disjunction of 4 conjunctions over 128 input variables. We again fix the sign parameter $\mathbf{s}$ to 0, as this aids in intepreting the result of the model, and we will show it does not significantly affect the rate of convergence.

3.1.1 Results

A good metric for the success of this model is the quality of the output of the neurosymbolic submodel. If we take the output distribution $\operatorname{softmax} \circ \psi_2 \circ m_1(\mathbf{x})$, and take the index of maximum probability as our true guess, comparing this to the actual categorisation over all images in the test dataset allows us to assess the quality of ψ_2. Interpretability requires that the parameters of ψ_2 be as crisp as possible, so we also consider the sum of the distances of all logical parameters from crisp values $0, 1$.

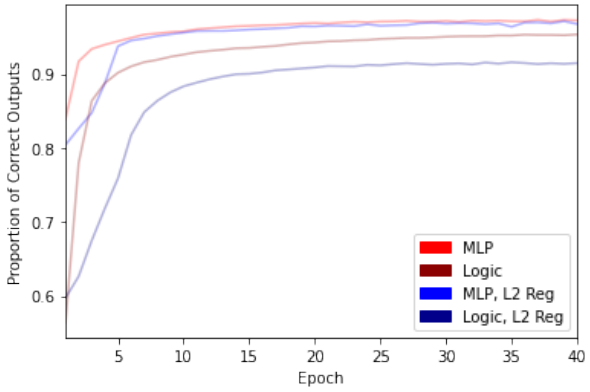

(a) Proportion of Correct Outputs (for both MLP and neurosymbolic paths).

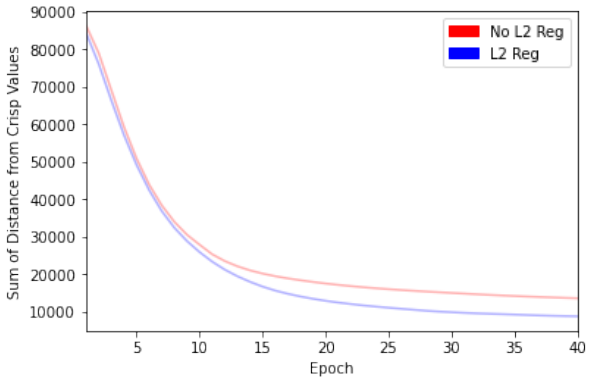

(b) Sum of distances from crisp parameters $0, 1$.

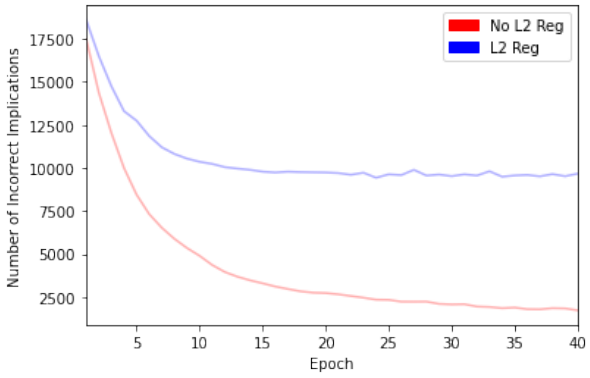

(c) Number of incorrect implications.

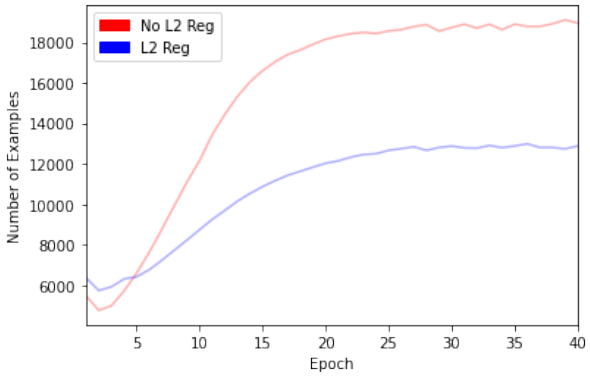

(d) Number of "example" implications.

Figure 3.1: Convergence of the MNIST categorisation model, $\delta = 10^{-1}$.

Figure 3.1 shows the results of optimising this model using Adam optimisation with a learning rate of 10^{-3}. We set $\delta = 10^{-1}$, and where ℓ_2 loss is used, $\lambda = 10^{-5}$. Figure 3.1a shows that the quality of predictions of the traditional MLP path does not degrade, achieving around 97% accuracy in both cases. Non-zero ℓ_2 regularisation diminishes the quality of the neurosymbolic prediction, but not significantly. Figure 3.1b shows that both models achieve relatively crisp parameters, with the average distance from $0, 1$ decreasing by a factor of 10.

Figure 3.1c and 3.1d measure the effectiveness of ψ_2 in capturing logical inference though the implication operator $\Rightarrow$. A single DNF in ψ_2 is a disjunction of conjunctions $c_1 \vee \cdots \vee c_n$, and we want this disjunction to be true if and only if the training data has the corresponding output y true. If this is the case, then for all conjunctions c_i, $c_i \Rightarrow y$. If, for some element of the test dataset $\mathbf{x}$, we have that c_i is true, but y is false, then our learnt conjunction is incorrect. If instead y is true, we can interpret c_i as *causing* y to be true. Figure 3.1c therefore represents the sum of $c_i \wedge \neg y$ over all conjunctions c_i and all test data pairs. Figure 3.1d represents the sum of $c_i \wedge y$ likewise. We see that the number of incorrect implications decreases over time, and the number of "example" implications increases, before both plateauing after around 20 epochs. ℓ_2 regularisation also diminishes the quality of both metrics, which is not surprising given the findings of 3.1a. In Appendix **??**, we further explore how varying the difference hyperparameter δ affects the quality of the resultant model.

3.2 Model Interpretation

The model we have designed has become quite adept at categorising MNIST images. The goal of this report, however, is to determine a method of interpreting said models. As before, we want to leverage the fact that a boolean statement in DNF can be considered a series of implications from conjunctions c to outputs y. It is interesting to note that statements $c \Rightarrow y$ are known as *Horn clauses*, and are a relatively small but highly expressive subset of boolean functions, which are widely used in symbolic learning algorithms, especially in ILP systems [28].

If for some DNF in ψ_2, the output y is true, and one of the antecedent conjunctions c is also true, then we interpret c as causing y. We therefore need only explain why c was true. In the model we have designed, c is the output of a generalised linear model, so we can use Variable Importance Measures (VIMs), as discussed in Section 1.2.

Figure 3.2 shows such an example. The listed features are elements of a conjunction c which implies the output that gives the image label 7. Each image is generated by taking the gradient of the output feature in $\mathbf{z}_1$ with respect to training image $\mathbf{x}$. The example shown is from the model with ℓ_2 hinge loss with hyperparameter $\lambda = 10^{-5}$. We can see that many of the features very closely map the shape of a number 7, and the remaining features capture small variances in said shape. This example was chosen as it required the conjunction with the fewest number of terms, more examples are given in Appendix **??**. Of note is that feature attributions are much more difficult to comprehend without ℓ_2 regularisation, as the model overfits to random noise around the borders of each image.

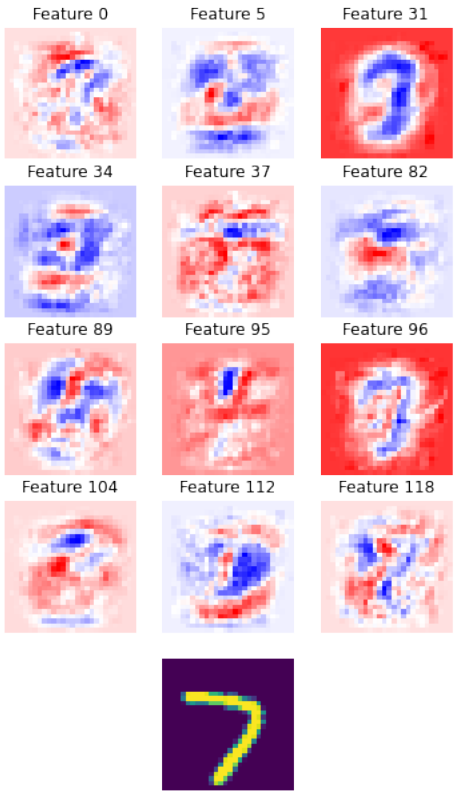

Figure 3.2: The image is given label 7 as all the above features are true.

Chapter 4

Conclusions

Chapter 5

Conclusions

Bibliography

[1] Rishabh Agarwal, Levi Melnick, Nicholas Frosst, Xuezhou Zhang, Ben Lengerich, Rich Caruana, and Geoffrey E Hinton. Neural additive models: Interpretable machine learning with neural nets. *Advances in Neural Information Processing Systems*, 34, 2021.

[2] Marco Ancona, Enea Ceolini, Cengiz Öztireli, and Markus Gross. *Gradient-Based Attribution Methods*, pages 169–191. Springer International Publishing, Cham, 2019.

[3] Dana Angluin and Philip Laird. Learning from noisy examples. *Machine Learning*, 2(4):343–370, 1988.

[4] Stephen H. Bach, Matthias Broecheler, Bert Huang, and Lise Getoor. Hinge-loss markov random fields and probabilistic soft logic. 2015.

[5] Supriyo Chakraborty, Richard Tomsett, Ramya Raghavendra, Daniel Harborne, Moustafa Alzantot, Federico Cerutti, Mani Srivastava, Alun Preece, Simon Julier, Raghuveer M. Rao, Troy D. Kelley, Dave Braines, Murat Sensoy, Christopher J. Willis, and Prudhvi Gurram. In *Interpretability of deep learning models: A survey of results*, 2017.

[6] Hanxiong Chen, Shaoyun Shi, Yunqi Li, and Yongfeng Zhang. Neural collaborative reasoning. In *Proceedings of the Web Conference 2021*. ACM, apr 2021.

[7] Li Deng. The mnist database of handwritten digit images for machine learning research. *IEEE Signal Processing Magazine*, 29(6):141–142, 2012.

[8] Hubert L Dreyfus. *What computers still can't do: A critique of artificial reason*. MIT press, 1992.

[9] Richard Evans and Edward Grefenstette. Learning explanatory rules from noisy data, 2017.

[10] Andrew D Gordon, Thomas A Henzinger, Aditya V Nori, and Sriram K Rajamani. Probabilistic programming. In *Future of Software Engineering Proceedings*, pages 167–181. 2014.

[11] Ramanathan Guha. Towards a model theory for distributed representations, 2014.

[12] Petr Hájek. *Metamathematics of fuzzy logic*, volume 4. Springer Science & Business Media, 2013.

[13] Geoffrey E. Hinton, Nitish Srivastava, Alex Krizhevsky, Ilya Sutskever, and Ruslan R. Salakhutdinov. Improving neural networks by preventing co-adaptation of feature detectors, 2012.

[14] Michael J Kearns and Umesh Vazirani. *An introduction to computational learning theory*. MIT press, 1994.

[15] Diederik P Kingma and Jimmy Ba. Adam: A method for stochastic optimization. *arXiv preprint arXiv:1412.6980*, 2014.

[16] Erich Peter Klement, Radko Mesiar, and Endre Pap. *Triangular norms*, volume 8. Springer Science & Business Media, 2013.

[17] George Klir and Bo Yuan. *Fuzzy Sets and Fuzzy Logic*, volume 4. Prentice hall New Jersey, 1995.

[18] Nada Lavrac and Saso Dzeroski. *Inductive Logic Programming*. 1994.

[19] Tomas Mikolov, Kai Chen, Greg Corrado, and Jeffrey Dean. Efficient estimation of word representations in vector space. *arXiv preprint arXiv:1301.3781*, 2013.

[20] Tomáš Mikolov, Wen-tau Yih, and Geoffrey Zweig. Linguistic regularities in continuous space word representations. In *Proceedings of the 2013 conference of the north american chapter of the association for computational linguistics: Human language technologies*, pages 746–751, 2013.

[21] Christoph Molnar, Giuseppe Casalicchio, and Bernd Bischl. In *Interpretable Machine Learning – A Brief History, State-of-the-Art and Challenges*. Springer International Publishing, 2020.

[22] Ali Payani and Faramarz Fekri. Inductive logic programming via differentiable deep neural logic networks, 2019.

[23] Danilo Rezende and Shakir Mohamed. Variational inference with normalizing flows. In *International conference on machine learning*, pages 1530–1538. PMLR, 2015.

[24] Matthew Richardson and Pedro Domingos. Markov logic networks. *Machine learning*, 62(1):107–136, 2006.

[25] Ryan Riegel, Alexander Gray, Francois Luus, Naweed Khan, Ndivhuwo Makondo, Ismail Yunus Akhalwaya, Haifeng Qian, Ronald Fagin, Francisco Barahona, Udit Sharma, et al. Logical neural networks. *arXiv preprint arXiv:2006.13155*, 2020.

[26] Luciano Serafini and Artur d'Avila Garcez. Logic tensor networks: Deep learning and logical reasoning from data and knowledge, 2016.

[27] Shaoyun Shi, Hanxiong Chen, Weizhi Ma, Jiaxin Mao, Min Zhang, and Yongfeng Zhang. Neural logic reasoning, 2020.

[28] Maarten H Van Emden and Robert A Kowalski. The semantics of predicate logic as a programming language. *Journal of the ACM (JACM)*, 23(4):733–742, 1976.

[29] Emile van Krieken, Erman Acar, and Frank van Harmelen. Analyzing differentiable fuzzy logic operators. *Artificial Intelligence*, 302:103602, 2022.

[30] Joel Vaughan, Agus Sudjianto, Erind Brahimi, Jie Chen, and Vijayan N. Nair. Explainable neural networks based on additive index models, 2018.

[31] Bing Xu, Naiyan Wang, Tianqi Chen, and Mu Li. Empirical evaluation of rectified activations in convolutional network, 2015.

[32] Lotfi A Zadeh. *Fuzzy sets, fuzzy logic, and fuzzy systems: selected papers*. World Scientific, 1996.